

H₂ self-shielding with non-LTE rovibrational populations: implications for cooling in protogalaxies

J. Wolcott-Green and Z. Haiman ^{*}

Department of Astronomy, Columbia University, 550 West 120th Street, MC 5246, New York, NY 10027, USA

ABSTRACT

The abundance of molecular hydrogen (H₂), the primary coolant in primordial gas, is critical for the thermodynamic evolution and star-formation histories in early protogalaxies. Determining the photodissociation rate of H₂ by an incident Lyman-Werner (LW) flux is thus crucial, but prohibitively expensive to calculate on the fly in simulations. The rate is sensitive to the H₂ rovibrational distribution, which in turn depends on the gas density, temperature, and incident LW radiation field. We use the publicly available CLOUDY package to model primordial gas clouds and compare exact photodissociation rate calculations to commonly-used fitting formulae. We find the fit from Wolcott-Green et al. (2011) is most accurate for moderate densities $n \sim 10^3 \text{ cm}^{-3}$ and temperatures, $T \sim 10^3 \text{ K}$, and we provide a new fit, which captures the increase in the rate at higher densities and temperatures, owing to the increased excited rovibrational populations in this regime. Our new fit has typical errors of a few percent up to $n \leq 10^7 \text{ cm}^{-3}$, $T \leq 8000 \text{ K}$, and H₂ column density $N_{\text{H}_2} \leq 10^{17} \text{ cm}^{-2}$, and can be easily utilized in simulations. We also show that pumping of the excited rovibrational states of H₂ by a strong LW flux further modifies the level populations when the gas density is low, and noticeably decreases self-shielding for $J_{21} > 10^3$ and $n < 10^2 \text{ cm}^{-3}$. This may lower the “critical flux” at which primordial gas remains H₂-poor in some protogalaxies, enabling massive black hole seed formation.

Key words: cosmology: theory – early Universe – galaxies: formation – molecular processes – stars: Population III

1 INTRODUCTION

It has long been known that the cooling of metal-free primordial gas, from which the first generation of stars form in protogalaxies, is dominated by H₂ molecules (Saslaw & Zipoy 1967). Once these first (“Population III”) stars begin to shine, however, the UV radiation they emit begins to photodissociate H₂ via the Lyman-Werner (LW) bands ($E_\nu = 11.1 - 13.6 \text{ eV}$). Photodissociation feedback is non-trivial to model, particularly when the H₂-column density becomes sufficiently high for it to become self-shielding ($N_{\text{H}_2} \gtrsim 10^{13} \text{ cm}^{-2}$). Accurate modeling is important because the thermodynamic and star formation histories in early protogalaxies depend sensitively on the H₂ abundance.

An example of this sensitivity occurs in the well-known “direct collapse” scenario, in which a protogalaxy may avoid fragmentation (and thereby Pop III star formation) if exposed to a sufficiently strong UV flux from a near neighbor (e.g. Regan et al. 2017, and references therein). In this case,

the H₂-abundance remains too low to cool below the virial temperature of the halo, preventing fragmentation on stellar scales. It has been proposed that the resulting rapid accretion possible in this scenario may lead to the formation of massive black holes ($M_{\text{BH}} \gtrsim 10^{4-5} M_\odot$) that seed the earliest quasars (see reviews by Volonteri 2010; Haiman 2013; Wise 2018). The predicted “critical” UV-flux to keep protogalactic [gas H₂-poor (commonly denoted J_{crit}) depends sensitively on the detailed calculation of the optically-thick H₂-photodissociation rate.

Calculating the full optically-thick photodissociation rate on the fly is prohibitively expensive in simulations due to the large number of LW transitions. There are a total of 301 rovibrational states of the ground electronic state (X) and over half a million allowed electronic transitions. Previous studies have relied, therefore, on fitting formulae for the optically-thick H₂ photodissociation rate provided by Draine & Bertoldi (1996). Their fit models the behavior well when primarily the ground (ortho and para) states of the molecule are populated. Alternatively, some studies use the modified fit provided by Wolcott-Green et al. (2011, hereafter WGH11), which is more accurate at higher den-

* E-mail: jemma@astro.columbia.edu; zoltan@astro.columbia.edu

sities and temperatures, when the rotational levels of the ground vibrational state are in, or close to, LTE.

Both of these approximations are gross simplifications of the true rovibrational level populations, which in general are time-dependent and sensitive to the gas density, temperature, and rate of UV excitation. As discussed in WGH11, the optically-thick rate can be quite sensitive to changes in the level populations, and in particular to the number of states that contribute to self-shielding, as more states becoming significantly populated reduces the effective self-shielding column density.

In this paper, we use the publicly available CLOUDY¹ package (Ferland et al. 2017) to calculate the H₂ rovibrational populations under conditions similar to those in a pristine protogalactic gas cloud irradiated by UV. We compare the resulting optically-thick photodissociation rate to that predicted by the commonly used fitting formulae. We find that the fitting formula provided by WGH11 is accurate in a narrow range of densities and temperatures ($n \approx 10^3 \text{ cm}^{-3}$ and a few $\times 10^3 \text{ K}$), and we provide an improved fitting formula that is accurate for a larger swath of the parameter space. In particular, our improved fit matches the true rate of only a few percent up to $T = 8000 \text{ K}$, $n = 10^7 \text{ cm}^{-3}$, $N_{\text{H}_2} = 10^{16} \text{ cm}^{-2}$, and with typical errors of order ten per cent up to higher column density, $N_{\text{H}_2} = 10^{17} \text{ cm}^{-2}$.

In the case of a protogalactic candidate for direct collapse, there is an additional modification to the rovibrational distribution and thus to the optically-thick H₂ photodissociation rate that may be important, and which has not been considered in this context previously. When irradiated in the UV, decays following electronic excitation populate excited rovibrational levels of the ground electronic state (X), which subsequently decay through infrared emission in a radiative cascade. In the presence of a very strong UV flux, the radiative cascade of the UV-pumped H₂ molecules can be interrupted by absorption of another UV photon. Shull (1978) found this “re-pumping” affects the radiative cascade $J_{21} \gtrsim 10^3$, and is *more likely* than decay of the molecule to a lower rovibrational state when the incident UV flux exceeds $J_{21} \sim 10^5$, with J_{21} defined in the usual way: $J_\nu = J_{21} \times 10^{-21} \text{ erg s}^{-1} \text{ cm}^{-2} \text{ sr}^{-1} \text{ Hz}^{-1}$.

We find in our CLOUDY models that pumping from excited rovibrational states, leading to reduced effective column density, can decrease self-shielding by up to an order of magnitude at fluxes as low as $J_{21} = \text{a few} \times 10^3$ when the density is low $n < 10^3 \text{ cm}^{-3}$. Importantly, this is similar to the common determinations of $J_{\text{crit},21} \sim 10^3$ (e.g. WGH11). At higher densities ($> 10^3 \text{ cm}^{-3}$), the rovibrational level populations tend toward their LTE values and we find there is no effect on the self-shielding behavior even for the strongest UV flux we consider, $J_{21} \sim 10^5$.

This paper is organised as follows: In § 2 we describe the details of our numerical modeling; in § 3 we discuss our results using a variety of CLOUDY models, and an updated fitting formulae for the optically-thick H₂ photodissociation rate. We summarize our results and offer conclusions in § 4.

2 NUMERICAL MODELING

2.1 Cloudy Models

We use the most recent version of the publicly available package CLOUDY (v17.01) to calculate the rovibrational level populations of H₂ in a gas of primordial composition and illuminated on one face (plane parallel geometry). We use a grid of densities and temperatures in the range $n = 10^{0-7} \text{ cm}^{-3}$ and $T = 500 - 10^5 \text{ K}$. We hold both constant in our models, in order to tease apart the effects on the rovibrational distribution and the resulting photodissociation rate.

We use the Draine & Bertoldi (1996) galactic background spectrum for the incident radiation in our fiducial models (see their Equation 23), but our results are not sensitive to this choice. If we use the Black & van Dishoeck (1987) interstellar radiation field instead, the photodissociation is nearly unchanged. (However, neither of these spectra have prior processing in the LW bands; Wolcott-Green et al. 2017 show that if the incident radiation originates from an older stellar population, absorption lines in the spectrum can change the resulting photodissociation rate by a factor of two or more.)

We use the “large H₂” model, details of which can be found in Shaw et al. (2005); this model resolves all 301 bound levels of the H₂ electronic ground state and six excited electronic states. Several thousand energy levels of the molecule and approximately 5×10^5 permitted transitions are included. In order to explore the results at high UV flux and low density, we decreased the threshold fractional abundance of H₂ at which the resolved populations are calculated (“H₂-to-H-limit” in CLOUDY) from its default (10^{-8}) to 10^{-12} .

2.2 The Rate Calculation

Photodissociation of H₂ occurs primarily via the two-step Solomon process, in which the molecule is first electronically pumped by a UV photon (11.1 – 13.6 eV) from the ground state $X^1\Sigma_g^+$ to the $B^1\Sigma_u^+$ (Lyman) or $C^1\Pi_u$ (Werner) states. The subsequent decay to the vibrational continuum results in dissociation ~ 15 per cent of the time. The “pumping rate” from a given rovibrational state (v, J) to an excited electronic state (v', J') is:

$$\zeta_{v,J,v',J'} = \int_{\nu_{\text{th}}}^{\nu_{13.6 \text{ eV}}} 4\pi\sigma_\nu \frac{J_\nu}{h_P\nu} d\nu, \quad (1)$$

where σ_ν is the frequency dependent cross-section and h_P is Planck’s constant. The frequency threshold, ν_{th} , corresponds to the lowest energy photons capable of efficiently dissociating H₂, with $h\nu = 11.18 \text{ eV}$. We do not include photons with energies above the Lyman limit, which are likely to have been absorbed by the neutral IGM at the relevant redshifts (prior to reionization). In the direct collapse scenario with irradiation from a bright neighbor, the escape fraction of ionizing photons may be small anyway (see e.g. Wise et al. 2014). Including $E > 13.6 \text{ eV}$ radiation would cause increased hydrogen ionization in the collapsing gas, which is not included in the present context.

The dissociation rate from a given (v, J) is the product of the pumping rate and the fraction of decays that result

¹ www.nublado.org

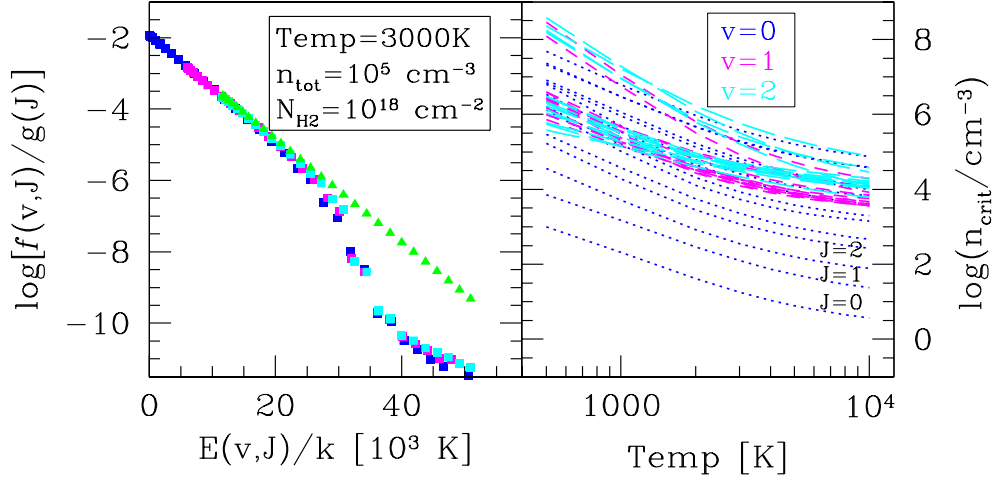


Figure 1. **Left** The fractional populations of H₂ in rovibrational states with $v = 0 - 2$ and energy $E_{v,J}$ predicted by the CLOUDY “Large H₂” model. Green triangles show the LTE populations while the resolved (non-LTE) populations in $v = 0, 1, 2$ are shown by dark blue, magenta, and cyan squares, respectively. **Right:** The temperature dependence of the critical density (for LTE) is shown for each of the states $v = (0 - 2), J$ (with dotted, short-dash, and long-dash lines, respectively.) As illustrated in this panel, $T = 3,000\text{K}$, $n = 10^5 \text{ cm}^{-3}$ exceeds the critical density of the lowest ~ 35 states, and the populations of these states, shown in the left-hand panel, are indeed near their LTE values, as expected.

in dissociation (summed over all excited states, v', J'):

$$k_{\text{diss},v,J} = \sum_{v',J'} \zeta_{v,J,v',J'} f_{\text{diss},v',J'} \quad (2)$$

The dissociation probabilities $f_{\text{diss},v',J'}$, are provided by Abgrall et al. 2000.

While CLOUDY outputs the optically-thick dissociation rate itself, we re-calculate the rate in order to remove the effect of HI shielding H₂ and isolate the self-shielding only. This also allows us to test the effects of changing one variable at a time, including the incident spectrum, the rovibrational distribution, and the temperature. WGH11 found that the total shielding of H₂ can be modeled with good accuracy by including a simple multiplicative factor that depends only on the HI column density: $f_{\text{shield,tot}}(N_{\text{H}_2}, N_{\text{HI}}, T) = f_{\text{shield}}(N_{\text{H}_2}) \times f_{\text{HI}}(N_{\text{HI}})$. Therefore, the effects we quantify for self-shielding are directly applicable to the total shielding, though HI is not included in our fiducial calculations.

We initiate the calculation with the CLOUDY incident spectrum at the irradiated face, and step through each discrete zone, summing the contributions to the frequency-dependent optical depth from the H₂ transitions. In each zone, we use the resolved rovibrational populations from CLOUDY, $f_{v,J}$. The total rate in a given zone is then:

$$k_{\text{diss}} = \sum_{v,J} k_{\text{diss},v,J} \times f_{v,J} \quad (3)$$

2.3 Critical Densities for LTE in H₂ Rovibrational States

One of the primary challenges in calculating the optically-thick photodissociation rate of H₂ is determining the rovibrational level population distribution. In the non-LTE case,

the distribution is time-dependent and sensitive to the gas temperature, density, as well as the UV pumping rate.

In a low-density gas, collisional de-excitation is slow and the radiative decay rates entirely determine the cascade to lower states; however, the radiative lifetimes are long enough that even at moderate densities collisional de-excitation begins to have an effect (Draine 2010). The lowest energy states ($v = 0, J$) reach LTE at critical densities of $n_{\text{H}} \lesssim 10 \text{ cm}^{-3}$ at $T = 10^4 \text{ K}$ (see Figure 1). The critical density for a given transition is:

$$n_c(u \rightarrow l) = \frac{A(u \rightarrow l)}{\gamma(u \rightarrow l)} \quad (4)$$

here $\gamma(u \rightarrow l)$ is the collisional de-excitation rate and $A(u \rightarrow l)$ is the spontaneous decay transition probability. Above the critical density, the fractional population of the state approaches its LTE value and is then dependent only on the temperature. Because $A(u \rightarrow l) \propto E_{\text{lu}}^5$ (where E_{lu} is the energy of the transition between upper and lower states), the critical density increases rapidly with J within a vibrational manifold while it decreases rapidly with temperature. Figure 1 shows the temperature dependence of the critical densities of the lowest energy levels ($v = 0 - 2, J$). We use the fitting formulae for the collisional rates provided by Le Bourlot et al. (1999), which do not include all of the highest energy levels, but are nonetheless useful for the present purpose.

The left panel of Figure 1 shows the H₂ fractional level populations ($v = 0 - 2, J$) determined by CLOUDY for a gas at $T = 3000\text{K}$ and $n = 10^5 \text{ cm}^{-3}$. Resolved (non-LTE) populations (squares) diverge from the LTE values (triangles) for states with energies above $E_{v,J}/k_{\text{B}} \sim 2 \times 10^4 \text{ K}$, for which the critical densities exceed $n = 10^5 \text{ cm}^{-3}$. In the right panel of this figure, we show the temperature dependence of the

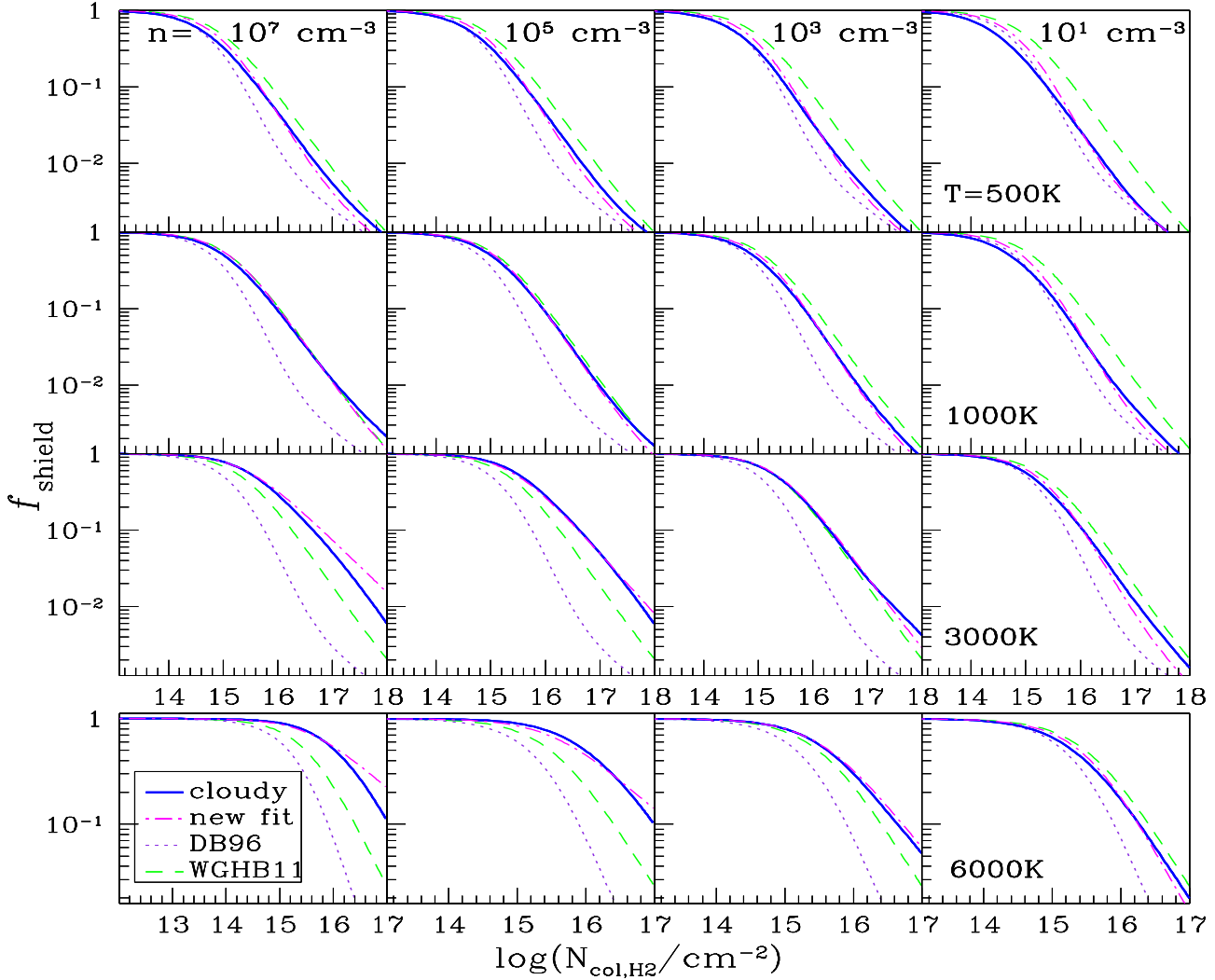


Figure 2. The optically-thick H_2 -photodissociation rate is shown, parameterized by the self-shielding factor, $f_{\text{shield}}(N_{\text{H}_2}, T) = k_{\text{LW}}(N_{\text{H}_2}, T)/k_{\text{LW}}(N_{\text{H}_2} = 0, T)$. Dark blue (solid) curves show results with fully-resolved rovibrational populations from CLOUDY models (at fixed density and temperature, as indicated on the figure). Green (dashed) and purple (dotted) curves show the fitting formulae for f_{sh} provided by Wolcott-Green et al. (2011) and Draine & Bertoldi (1996), respectively. Magenta (dot-dash) curves show results of the more accurate revised fitting formula in Equations 7-8.

critical density for the same states $v = (0 - 2), J$. From this figure, we see that the critical densities of the lowest ~ 35 states are less than $n = 10^5 \text{ cm}^{-3}$ at $T = 3000\text{K}$, and the populations of these states (shown in the left panel) are indeed near their LTE values, as expected.

2.4 Analytical Fitting Formulae for the Shielding Factor

Because of the computational expense of calculating the full optically-thick H_2 -photodissociation rate, several analytic fits have been suggested, parameterized by a “shielding factor:”

$$f_{\text{shield}}(N_{\text{H}_2}, T) = k_{\text{diss}}(N_{\text{H}_2}, T)/k_{\text{diss}}(N_{\text{H}_2} = 0, T). \quad (5)$$

Draine & Bertoldi (1996) (hereafter DB96) provided two useful fitting formulae for this purpose, the more accurate

of which (their equation 37) has the form:

$$f_{\text{shield,DB}}(N_{\text{H}_2}, T) = \frac{0.965}{(1 + x/b_5)^\alpha} + \frac{0.035}{(1 + x)^{0.5}} \times \exp[-8.5 \times 10^{-4} (1 + x)^{0.5}]. \quad (6)$$

DB96 set $\alpha = 2$, $x \equiv N_{\text{H}_2}/5 \times 10^{14} \text{ cm}^{-2}$, $b_5 \equiv b/10^5 \text{ cm s}^{-1}$, where b is the Doppler broadening parameter.

WGBH11 showed that this fit is only accurate for low-density gas at temperatures of \sim a few hundred K. They modified it by setting $\alpha = 1.1$ in order to better fit the population results in gas at \sim a few thousand Kelvin and densities $\sim 10^3 \text{ cm}^{-3}$ —relevant for a gravitationally-collapsing protogalactic halo. With this modification, self-shielding is weaker than the original DB96, appropriate for H_2 populations that are spread out over more (v, J) states, as explained above.

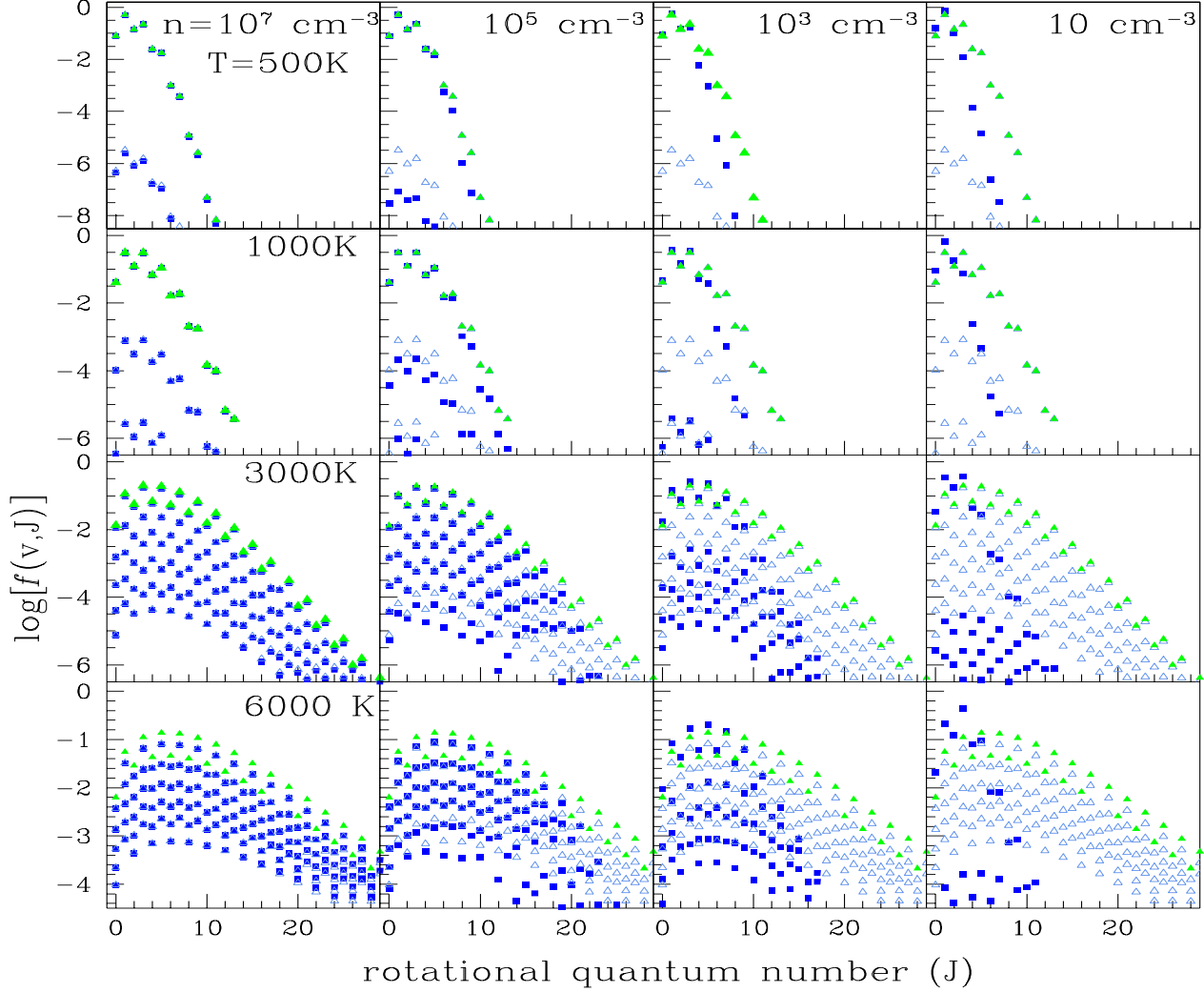


Figure 3. The fractional populations of H_2 in our CLOUDY models are shown for each rovibrational state (v_15, J) . Dark blue squares are used for the fully-resolved (non-LTE) results while grey (open) triangles are the full LTE populations. Green (filled) triangles show a Boltzmann distribution for populations in the ground vibrational state only $v = 0$, which was the basis for a commonly used fitting formulas for f_{shield} provided by Wolcott-Green et al. (2011).

3 RESULTS AND DISCUSSION

3.1 How accurate are fitting formulae for f_{shield} ?

With our CLOUDY models, we can evaluate the accuracy of the DB96 and WGHB11 fits compared to the “true” photodissociation rate over a wide swath of the parameter space. We include higher densities ($n \leq 10^7 \text{ cm}^{-3}$) and temperatures ($T \leq 8000\text{K}$) than in those previous studies, so that we can quantify the changes in the rate when the excited vibrational states become populated and eventually reach LTE. WGHB11 considered gas with density up to only $n \lesssim 10^3 \text{ cm}^{-3}$, and the DB96 fits were designed for much lower temperatures, $T \sim 100\text{K}$.

In Figure 2 we show our f_{shield} results in CLOUDY models with low flux $J_{21} = 0.1$ (dark blue curves). The DB96 fitting formula (gray curves) significantly overestimates shielding compared to CLOUDY at all but the lowest temperatures

and densities ($T = 500\text{K}, n = 10 \text{ cm}^{-3}$), as expected. The WGHB11 fit (green dashed curves) is more accurate up to higher temperature and density $T \approx 3000\text{K}, n \approx 10^3 \text{ cm}^{-3}$; however, it also gives f_{shield} that is far too small (underestimates the actual photodissociation rate) at $T > 3000\text{K}, n > 10^3 \text{ cm}^{-3}$. While this regime may not be relevant for the direct-collapse scenario, in which the gas thermodynamic evolution is determined at lower density $n \sim 10^2$, it could be important for simulations of “Pop III” star formation in the presence of a strong incident UV flux.

Figure 3 shows the origin of the discrepancy of the WGHB11 fit. The resolved level populations for each of the CLOUDY models (dark blue squares) are shown in comparison to the predicted LTE populations (light blue triangles). The WGHB11 fit was based on a Boltzmann distribution *only in the ground vibrational state*, shown in the figure by green triangles. This $v = 0$ model is a good approximation up to

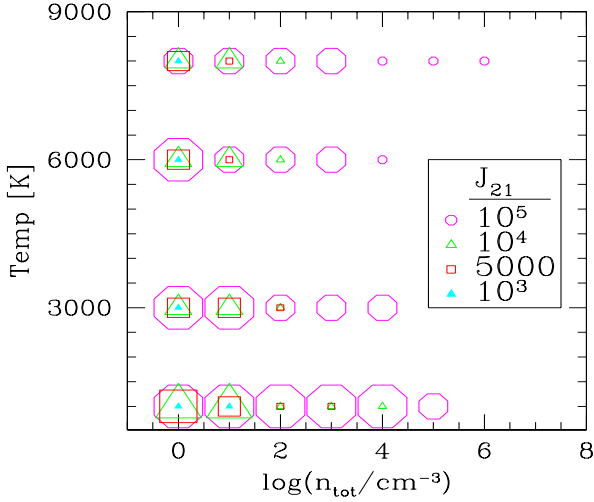


Figure 4. The densities and temperatures of CLOUDY models in which the a strong UV flux increases the optically-thick H_2 photodissociation rate by more than a threshold factor x are shown for three threshold values $x = 1.25, 2, 10$ with small, medium, and large (circles) respectively. Results with four UV-intensities are shown, as indicated in the figure legend.

$T \sim 3000\text{K}$. At higher temperatures and densities, however, the populations in $v > 0$ states increase. Because the number of populated states is what matters for f_{shield} – a greater number of populated states leads to lower effective column density for shielding – the $v = 0$ assumption for f_{shield} is erroneously small.

3.2 A New Fitting Formula for f_{shield}

In order to find a more accurate fitting formula for f_{shield} , we need to increase the sensitivity to temperature for densities above $n > 10 \text{ cm}^{-3}$, reflecting the strong temperature dependence of the critical densities.

We make use of the original form provided by DB96, which WGH11 modified with a new factor α . Here, we introduce a density and temperature dependence of α , so that the effect of spreading populations over more levels at high n/T is captured:

$$f_{\text{shield}}(N_{\text{H}_2}, T) = \frac{0.965}{(1 + x/b_5)^{\alpha(n,T)}} + \frac{0.035}{(1 + x)^{0.5}} \times \exp[-8.5 \times 10^{-4} (1 + x)^{0.5}]. \quad (7)$$

$$\begin{aligned} \alpha(n, T) &= A_1(T) \times \text{dexp}(-c_1 \times \log(n/\text{cm}^{-3})) + A_2(T) \\ A_1(T) &= c_2 \times \log(T/\text{K}) - c_3 \\ A_2(T) &= -c_4 \times \log(T/\text{K}) + c_5 \end{aligned} \quad (8)$$

The best fit parameters, optimized using the AMOEBA routine in Numerical Recipes (Press et al. 1993), are as follows: $c_1 = 0.2856$, $c_2 = 0.8711$, $c_3 = 1.928$, $c_4 = 0.9639$, $c_5 = 3.892$. The accuracy of the new fit is improved over the entire parameter space compared to the previous fits, as shown in Figure 2, with typical errors of a few percent for f_{shield} up to $N_{\text{H}_2} = 10^{17} \text{ cm}^{-2}$.

It is worth noting that Richings et al. (2014) also used CLOUDY models similar to ours to investigate the accuracy of various fitting formulae compared to the “true” optically-thick rate. However, in that study, the true rate is calculated by CLOUDY itself, which includes HI-shielding of H_2 along with self-shielding. Therefore, their results are particular to those CLOUDY models and their specific HI/ H_2 profiles. As a result, we have not compared our results to the fitting formula they provide.

3.3 Is pumping important at the relevant flux strength?

In order to quantify the effect of a strong incident UV flux on the optically-thick H_2 -photodissociation rate in a primordial cloud, we have run a grid of CLOUDY models with a range of flux intensities, $J_{21} = (0.1, 10^5)$, gas temperatures, $T = (500, 8000)\text{K}$, and densities $n = 10^{0-7} \text{ cm}^{-3}$. In Figure 4 we show the combinations for which a strong flux changes the shielding by more than a threshold factor $f_{\text{shield}}(J_{21})/f_{\text{shield}}(J_{21} = 0.1) > x$, for three threshold values $x = 1.25, 2, 10$. Our results are shown if the above criterion is fulfilled at any column density up to $N_{\text{H}_2} = 10^{17} \text{ cm}^{-2}$.

In the majority of cases, there is no significant change in the self-shielding except at very high intensity, $J_{21} = 10^5$. However, at low densities $n \leq 10^2 \text{ cm}^{-3}$, even a “moderate” UV intensity increases the dissociation rate. For example, an incident flux of only $J_{21} = 5,000$ reduces shielding by a factor > 2 for a gas $n = 10 \text{ cm}^{-3}$ and by more than an order of magnitude when $n = 1 \text{ cm}^{-3}$. Even a flux of just $J_{21} = 10^3$ leads to a 40–50 per cent decrease in the shielding in the lowest density cases $n \leq 10 \text{ cm}^{-3}$.

Why is there a pronounced difference in self-shielding in the low-density, high-flux cases? Figure 5 shows the origin of this effect. The fractional populations of the H_2 rovibrational levels are shown, in the left-hand panel in both the strong- and weak-UV cases, for a low density CLOUDY model ($n = 10 \text{ cm}^{-3}$). Because pumping has the greatest effect near the edge of the cloud, where there is the least shielding, we show the level populations *at the irradiated face*. In the strong-UV case (magenta open triangles), many excited states $v > 0$ are populated. This is to be expected for a low-density gas, wherein strong UV pumping leads to a radiative cascade through excited states that are not populated by collisional processes alone. In contrast, in the weak-UV case, (green circles) only a few states are populated. We also show the cumulative populations (blue filled triangles) in the strong-UV case, which are nearly identical to those with weak-UV. This illustrates that pumping does not affect the bulk populations, as is expected due to shielding.

As discussed above, the spreading out of H_2 column density in more (v, J) states by pumping decreases the effective self-shielding column density, since each molecule “sees” fewer molecules in the same (v, J) state between it and the irradiated face of the cloud. The right panel of Figure 5 shows the “pumped” shielding factor $f_{\text{shield}}(J_{21} = 5,000)$ is three times larger than for small J_{21} at $N_{\text{H}_2} = 10^{17} \text{ cm}^{-2}$. With $J_{21} = 10^5$, the optically-thick photodissociation rate is \sim an order of magnitude larger than the same for small J_{21} . At $J_{21} = 10^3$, the largest change in the shield factor is ~ 40 per cent at $N_{\text{H}_2} \sim$ a few $\times 10^{15} \text{ cm}^{-2}$. In both panels of Figure

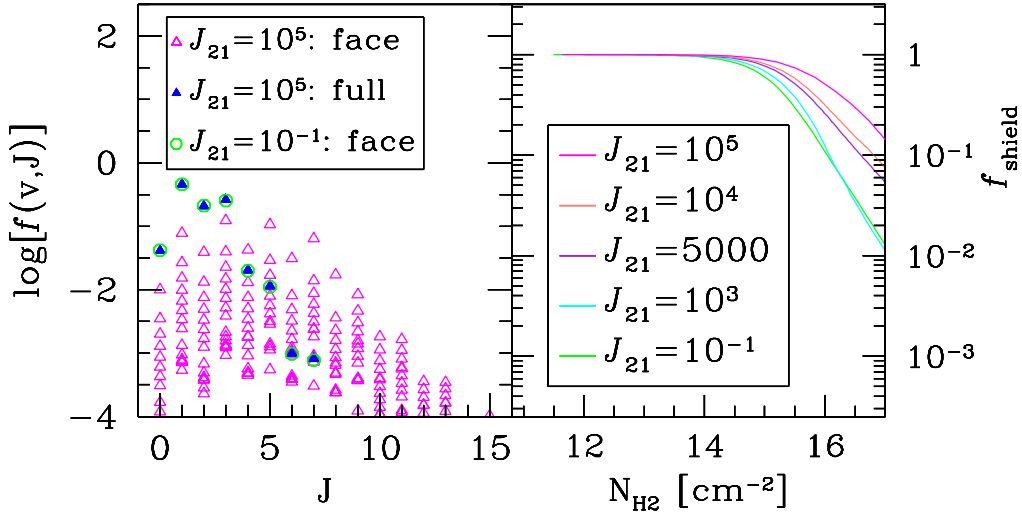


Figure 5. Left: The fractional population of H₂ in rovibrational states (v, J) are shown for two different CLOUDY models with the same temperature (T = 6000K) and density (n = 1 cm⁻³). Blue (filled) triangles show the cumulative populations of a cloud with N_{H2} = 10¹⁷ cm⁻² and irradiated by a strong-UV flux (J₂₁ = 10⁵, in the usual units). Magenta (open) triangles show only the populations at the illuminated face of the same cloud. Green (open) circles show the populations at the face of a cloud irradiated by a much weaker UV flux (J₂₁ = 0.1). The panel shows that significant UV-pumping of excited rovibrational states occurs at the illuminated face, while the populations deeper in the cloud are unaffected by the strong incident UV flux. **Right:** the optically-thick photodissociation rate, parameterized by a shield factor f_{shield}, at varying UV flux levels (see legend). As expected for the strong-UV case (J₂₁ = 10⁵), self-shielding is weaker due to pumping of H₂ to a larger number of rovibrational states, while at J₂₁ = 10³, the shielding is much closer to the “no-pumping” case (J₂₁ = 0.1). As in the left panel, the CLOUDY models have constant temperature T = 6000K and density n = 1 cm⁻³.

5, all of the CLOUDY models have constant T = 6000K and n = 1 cm⁻³.

In higher density models, n > 10³ cm⁻³, there is no pumping effect on the H₂ rovibrational populations. This is because the populations in the first few vibrational states (the most important for self-shielding) are already tending toward (or in) LTE at these densities (see Figure 3). In addition, larger neutral hydrogen column densities likely decrease the UV pumping more in these higher density cases, even near the illuminated face of the cloud.

It is worth noting that the density/temperature/J₂₁ space where pumping modifies the self-shielding behavior is very similar to that relevant for determining the critical flux to keep the halo H₂-poor, and thus for potential direct collapse to a supermassive-black hole seed. For example, Omukai (2001); Shang et al. (2010), show that the bifurcation in the cooling history of DCBH candidate halos occurs when collapsing gas reaches n ~ 10² cm⁻³ and T = 8000K and the critical flux is J₂₁ ~ 10³⁻⁴ (WGBH11 and references therein). Therefore, it is likely that weaker shielding caused by UV-pumping at densities n = 10⁰⁻² cm⁻³ is indeed relevant in the direct-collapse case, and pumping may well lead to a *smaller* J_{crit} if accounted for in simulations.

4 CONCLUSIONS

Using CLOUDY non-LTE models of pristine gas, we calculate the optically-thick H₂ photodissociation rate using the

resolved level populations and compare to the fitting formulae most commonly used in simulations. We find that the formula provided by Wolcott-Green et al. (2011) is most accurate at moderate densities, n ≲ 10³ cm⁻³, but fails to capture the weakening of shielding at higher densities and temperatures, when the populations in v > 0 tend to LTE. We provide a new modification to the fitting formula that increases its accuracy at all densities and temperatures and is a good fit up to n ~ 10⁷ cm⁻³, T = 8000K, N_{H2} = 10¹⁷ cm⁻². This new analytical fit can be easily used in simulations and one-zone models to better approximate the optically-thick photodissociation rate.

We also find that the photodissociation rate can be significantly increased in the presence of a strong UV flux, J₂₁ ≳ a few × 10³ due to pumping of molecules to excited rovibrational states. Increasing the number of populated states decreases the effective self-shielding column density that each molecule “sees,” and thus increases the optically-thick rate. This effect occurs only in gas at relatively low densities, n ≤ 10² cm⁻³, which happen to be similar to those important for the determination of J_{crit} for direct-collapse black hole formation. We find shielding is decreased by as much as an order of magnitude in some cases for an incident flux J₂₁ ~ 10⁴, and even a flux as low as J₂₁ ~ 10⁴ can cause a change > 40 per cent in some cases.

ACKNOWLEDGMENTS

We thank Gargi Shaw for assistance with the “Large H₂” model in CLOUDY and Greg Bryan for useful discussions. ZH acknowledges support from NASA grant NNX15AB19G. JWG acknowledges support from the NSF Graduate Research Fellowship Program.

REFERENCES

- Abgrall H., Roueff E., Drira I., 2000, *A&AS*, 141, 297
 Black J. H., van Dishoeck E. F., 1987, *ApJ*, 322, 412
 Draine B., 2010, in *Physics of the Interstellar and Inter-galactic Medium Molecular Hydrogen*. pp 346–351
 Draine B. T., Bertoldi F., 1996, *ApJ*, 468, 269
 Ferland G. J., Chatzikos M., Guzmán F., Lykins M. L., van Hoof P. A. M., Williams R. J. R., Abel N. P., Badnell N. R., Keenan F. P., Porter R. L., Stancil P. C., 2017, *Rev. Mex. Astron. Astrofis*, 53, 385
 Haiman Z., 2013, in Wiklind T., Mobasher B., Bromm V., eds, *Astrophysics and Space Science Library Vol. 396 of Astrophysics and Space Science Library, The Formation of the First Massive Black Holes*. p. 293
 Le Bourlot J., Pineau des Forêts G., Flower D. R., 1999, *MNRAS*, 305, 802
 Omukai K., 2001, *ApJ*, 546, 635
 Press W. H., Teukolsky S. A., Vetterling W. T., Flannery B. P., Lloyd C., Rees P., 1993, *The Observatory*, 113, 214
 Regan J. A., Visbal E., Wise J. H., Haiman Z., Johansson P. H., Bryan G. L., 2017, *Nature Astronomy*, 1, 0075
 Richings A. J., Schaye J., Oppenheimer B. D., 2014, *MNRAS*, 442, 2780
 Saslaw W. C., Zipoy D., 1967, *Nature*, 216, 976
 Shang C., Bryan G. L., Haiman Z., 2010, *MNRAS*, 402, 1249
 Shaw G., Ferland G. J., Abel N. P., Stancil P. C., van Hoof P. A. M., 2005, *ApJ*, 624, 794
 Shull J. M., 1978, *ApJ*, 219, 877
 Volonteri M., 2010, *Nature*, 466, 1049
 Wise J. H., 2018, *ArXiv e-prints*
 Wise J. H., Demchenko V. G., Halicek M. T., Norman M. L., Turk M. J., Abel T., Smith B. D., 2014, *MNRAS*, 442, 2560
 Wolcott-Green J., Haiman Z., Bryan G. L., 2011, *MNRAS*, 418, 838
 Wolcott-Green J., Haiman Z., Bryan G. L., 2017, *MNRAS*, 469, 3329